NASA Technical Memorandum 81501

# TIME DEPENDENT DIFFERENCE THEORY FOR SOUND PROPAGATION IN AXISYMMETRIC DUCTS WITH PLUG FLOW

K. J. Baumeister
Lewis Research Center
Cleveland, Ohio

Prepared for the
Sixth Aeroacoustics Conference
sponsored by the American Institute of Aeronautics
and Astronautics
Hartford, Connecticut, June 4-6, 1980

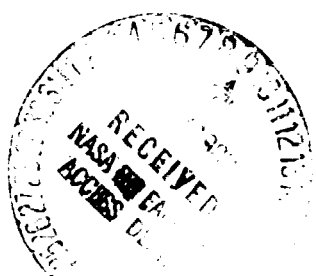

# TIME DEPENDENT DIFFERENCE THEORY FOR SOUND PROPAGATION IN AXISYMMETRIC DUCTS WITH PLUG FLOW

K. J. Baumeister
National Aeronautics and Space Administration
Lewis Research Center
Cleveland, Ohio 44135

## Abstract

The time dependent governing acoustic-difference equations and boundary conditions are developed and solved for sound propagation in an axisymmetric (cylindrical) hard wall duct with a plug mean flow and spinning acoustic modes. The analysis begins with a harmonic sound source radiating into a quiescent duct. This explicit iteration method then calculates stepwise in real time to obtain the transient as well as the "steady" state solutions of the acoustic field. The time dependent finite difference analysis has two advantages over the steady state finite difference and finite element techniques: (1) the elimination of large matrix storage requirements, and (2) shorter solution times under most conditions.

## Nomenclature

| | |
|---|---|
| A | $(\Delta r^2/\Delta x\Delta t)\eta_r M$ |
| $a_q$ | cell coefficient |
| B | $2(\Delta r/\Delta t)^2\eta_r^2 M/\zeta_M$ |
| $b_q$ | cell coefficient |
| $C_o^*$ | ambient speed of sound, m/s |
| $c_q$ | cell coefficient sound |
| $d_q$ | cell coefficient |
| E | $(\Delta r^2/\Delta x\Delta t)\eta_r(1-M^2)/\zeta_M$ |
| $e_q$ | cell coefficient |
| $f^*$ | frequency, Hz |
| $f_q$ | cell coefficient |
| $g_q$ | cell coefficient |
| $h_q$ | cell coefficient |
| I | number of axial grid points |
| i | $\sqrt{-1}$ |
| $i_q$ | cell coefficient |
| J | number of transverse grid points |
| $J_m$ | Bessel function |
| $L^*$ | length of duct, m |
| M | Mach number |
| m | spinning mode number |
| P | time-dependent dimensionless acoustic pressure, $P(x,r,t)$, $P^*/\rho_o^* c_o^{*2}$ |
| $P_m$ | time-dependent dimensionless acoustic pressure associated with m mode |
| P' | time-dependent dimensionless acoustic pressure with angular variations, $P'(x,r,\theta,t)$, $P'^*/\rho_o^* c_o^{*2}$ |
| p | spatially dependent "steady" acoustic pressure, $p(x,r)$ |
| $p_{m,n}$ | analytical solution for m spinning mode and n radial mode |
| r | radial coordinate, $r^*/r_o^*$ |
| $r_o^*$ | radius of duct, m |
| $\Delta r$ | radial grid spacing |
| $T^*$ | period, $1/f^*$, s |
| t | dimensionless time, $t^*/T^*$ |
| $\Delta t$ | time step |
| U | axial acoustic velocity, $u^*/c_o^*$ |
| x | axial coordinate, $x^*/r_o^*$ |
| $\Delta x$ | axial grid spacing |
| $\alpha$ | eq. (18) |
| $\alpha_{m,n}$ | eigenvalue |
| $\beta$ | eq. (12) |
| $\zeta_e$ | specific acoustic impedance at exist |
| $\zeta_M$ | $\zeta_e(1+M/\zeta_e)$ |
| $\eta_r$ | dimensionless frequency, $r_o^* f^*/c_o^*$ |
| $\lambda$ | dimensionless axial wavelength |
| $\theta$ | angular coordinate |
| $\rho_o^*$ | ambient air density, $kg/m^3$ |
| $\Psi$ | eq. (19) |
| $\omega$ | angular frequency |

Subscripts

| | |
|---|---|
| e | exit condition |
| i | axial index (fig. 1) |
| j | radial index (fig. 1) |
| k | cell index |
| m | spinning mode number |
| n | radial mode number |
| o | ambient condition |

Superscripts

| | |
|---|---|
| * | dimensional quantity |
| k | time step |
| (1) | real part |
| (2) | imaginary part |

## Introduction

Both finite difference and finite element numerical techniques have been developed to study sound propagation with axial variations in Mach number, wall impedance, and duct geometry. Generally, the numerical solutions have been limited to low frequency sound and short ducts, because many grid points or elements were required to resolve the axial wavelength of the sound. For plane wave propagation, the number of axial grid points or elements is directly proportional to the sound frequency and duct length[1] (eq. (77)), and inversely proportional to one minus the Mach number.[2] This later dependence also severely limits the appli-

cation of numerical techniques for high Mach number inlets.

Customarily, the pressure and acoustic velocities are assumed to be simple harmonic functions of time. In this case, the time independent wave equations can be used.[3] The matrices associated with the numerical solution to the time independent equations (called steady state solutions herein) must be solved exactly using such methods as Gauss elimination. As a result, large arrays of matrix elements must be stored. In an unpublished word at NASA Lewis Research Center by the author using reference 4, as well as in work of Quinn[5] (p. 3), the matrix has been modified to allow iteration techniques; unfortunately, the convergence is too slow to be of any practical value. Other approaches, such as in reference 6, might still allow the use of iteration methods.

Some special techniques have been developed to overcome the difficulties of high frequency, long ducts, and high Mach numbers. As shown in references 7 and 8, the wave envelope numerical technique can reduce the required number of grid points by an order of magnitude. In reference 9, this technique was used to optimize multielement liners of long lengths at high frequencies. At the present time, this technique has been applied only to the simple cases of no flow and plug flow. A numerical spatial marching technique was also developed in references 10 and 11. Compared to the standard finite difference or finite element boundary value approaches, the numerical marching technique is orders of magnitude shorter in computational time and required computer storage. The marching technique is limited to high frequencies and to cases where reflections are small.

A comprehensive literature summary of other time independent finite difference and finite element techniques is given elsewhere.[12,13]

As an alternative to the previously developed steady state theories, time dependent numerical solutions were developed for noise propagation in a two dimensional duct without flow[12] and with parallel sheared mean flow.[13] Advantageously, matrix storage requirements are significantly reduced in the time dependent analysis. The analysis began with a noise source radiating into an initially quiescent duct. Next, an explicit iteration method calculated stepwise in real time to obtain the transient as well as the "steady" state solution of the acoustic field. This time marching technique was found to be stable for both no flow and plug flow. The time dependent analysis was found to be superior to the steady state finite difference and finite element techniques because of much shorter solution times and the reduction of matrix storage requirements. Also because matrix manipulation is not required, the time-dependent approach is simpler to program and debug.

In the present paper, the time dependent technique developed in reference 12 will be extended to an axisymmetric (cylindrical) geometry with spinning acoustic modes and plug flow. First, the governing acoustic equations and boundary conditions are presented. Next, the governing acoustic-difference equations are derived. Immediately following the mathematical development, numerical examples are presented and compared with the corresponding steady state analytical results.

## Governing Equations and Boundary Conditions

The propagation of sound in an axisymmetric cylindrical hard wall duct, as shown in figure 1, is described by the wave equation and appropriate impedance boundary conditions.

### Wave Equations

The wave equation in a circular duct with a mean flow can be expressed in dimensionless form as

$$\eta_r^2 \frac{\partial^2 p'}{\partial t^2} = (1 - M^2) \frac{\partial^2 p'}{\partial x^2} + \frac{\partial^2 p'}{\partial r^2} + \frac{1}{r} \frac{\partial p'}{\partial r} + \frac{1}{r^2} \frac{\partial^2 p'}{\partial \theta^2} - 2\eta_r M \frac{\partial^2 p'}{\partial x \partial t} \qquad (1)$$

These and other symbols are defined in the nomenclature. The dimensionless frequency $\eta_r$ is defined as

$$\eta_r = \frac{r_o^*}{2\pi} \frac{\omega^*}{c_o^*} = \frac{r_o^* f^*}{c_o^*} \qquad (2)$$

The asterisks denotes dimensional quantities. In many other references, the characteristic length used in the definition of $\eta$ is often the duct diameter.

Because of the rotational nature of the rotor blades on a typical turbofan jet engine, large circumferential variations in acoustic pressure will occur depending on blade number and engine rpm. A three dimensional solution for sound propagation, however, would be expensive to perform. Customarily, since the equations are linear, the circumferential acoustic pressure variations are decomposed into spinning modes m:

$$p'(x,r,\theta,t) = \sum_m p_m(x,r,t) e^{im\theta} \qquad (3)$$

The summation is over those modes that are likely to occur in a partical applications. Considering solutions with a single spinning lobe number m,

$$p'(x,r,\theta,t) = p(x,r,t) e^{im\theta} \qquad (4)$$

the wave equation (1) reduces to

$$\eta_r^2 \frac{\partial^2 p}{\partial t^2} = (1 - M^2) \frac{\partial^2 p}{\partial x^2} + \frac{\partial^2 p}{\partial r^2} + \frac{1}{r} \frac{\partial p}{\partial r} - \frac{m^2}{r^2} p - 2\eta_r M \frac{\partial^2 p}{\partial x \partial t} \qquad (5)$$

Equation (5) in difference form will be solved to determine the pressure in the duct.

### Hard Wall Boundary Condition

The boundary condition at the surface of a hard wall duct is

$$\frac{\partial p}{\partial r} = 0 \qquad (6)$$

Entrance Condition

The boundary condition at the source plane $P(o,r,t)$ will be assumed to vary as $e^{i\omega^* t^*}$ or in a dimensionless form as $e^{i2\pi t}$. Furthermore, the transverse pressure variation (r-direction) will be assumed to correspond to the eigen functions $Jm(\alpha_{m\ n}r)$ associated with mode propagation in an infinitely long hard wall duct. The eigenvalues associated with mode (m,n) are tabulated in reference 14, p. 511 and reference 15, p. 411. Therefore, the source boundary condition used herein is

$$P(o,r,t) = J_m(\alpha_{m\ n}r)e^{i2\pi t} \tag{7}$$

Exit Impedance

The boundary condition at the exit of the duct can be expressed in terms of a specific acoustic impedance defined as

$$\zeta_e = \frac{P}{U} \tag{8}$$

The equation governing the acoustic velocity U is the usual linearized momentum equation:

$$\frac{\partial U}{\partial t} = -\frac{1}{\eta_r}\frac{\partial P}{\partial x} - \frac{M}{\eta_r}\frac{\partial U}{\partial x} \tag{9}$$

Substituting equation (8) into equation (9) yields:

$$\frac{\partial P}{\partial x} = -\frac{\eta_r}{\zeta_e(1 + M/\zeta_e)}\frac{\partial P}{\partial t} = -\frac{\eta_r}{\zeta_M}\frac{\partial P}{\partial t} \tag{10}$$

In equation (10), $\zeta_e$ has been assumed to be the impedance associated with mode propagation down an infinite duct. For transmission of a single acoustic mode without reflection, the exit impedance is[16]

$$\zeta_e = \frac{1 - M\beta}{\beta - M} \tag{11}$$

where

$$\beta = \sqrt{1 - \left(\frac{\alpha_{m\ n}}{2\pi\eta_r}\right)^2 (1 - M^2)} \tag{12}$$

Finally, the term $\partial^2 P/\partial x \partial t$ in the wave equation will also be evaluated at the duct exit. Differentiating equation (10) with time yields:

$$\frac{\partial^2 P}{\partial t \partial x} = -\frac{\eta_r}{\zeta_M}\frac{\partial^2 P}{\partial t^2} \tag{13}$$

Centerline Condition

The difference equation will be developed for modes with m equal or greater than 1. In these cases, the pressure at the centerline is equal to zero:

$$P(x,o,t) = 0 \qquad m \geq 1 \tag{14}$$

Initial Condition

For times equal to or less than zero, the duct is assumed quiescent, that is, the acoustic pressure is taken to be zero. For times greater than zero, the application of the noise source (eq. (7)) will drive the pressures in the duct.

Complex Notation

Because of the introduction of complex notation for the noise source, the acoustic pressure P is complex. The superscript (1) will represent the real term while (2) will represent the imaginary term.

$$P = P^{(1)} + iP^{(2)} \tag{15}$$

Difference Equations

Instead of a continuous solution in space and time, the finite-difference approximations will determine the pressure at isolated grid points in space as shown in figure 1, and at discrete time steps $\Delta t$. Starting from the known initial conditions at $t = 0$ and the boundary conditions, the finite-difference algorithm will march-out the solution to later times.

Central Region (Cell No. 1)

Away from the duct boundaries, in Cell no. 1 of figure 1, the second and first derivatives in the wave equation (eq. (5)) can be represented by the usual central differences in time and space[16] (p. 884)

$$\eta_r^2\left(\frac{P^{k+1}_{i,j} - 2P^k_{i,j} + P^{k-1}_{i,j}}{\Delta t^2}\right) = (1 - M^2)\left(\frac{P^k_{i+1,j} - 2P^k_{i,j} + P^k_{i-1,j}}{\Delta x^2}\right) + \left(\frac{P^k_{i,j+1} - 2P^k_{i,j} + P^k_{i,j-1}}{\Delta r^2}\right) - \frac{1}{r_j}$$

$$\times\left(\frac{P^k_{i,j+1} - P^k_{i,j-1}}{2\Delta r}\right) - \frac{m^2}{r_j^2}P^k_{i,j} - 2\eta_r M\left(\frac{P^{k+1}_{i,j} + P^k_{i-1,j} + P^k_{i+1,j} + P^{k-1}_{i,j} - 2P^k_{i,j} - P^{k+1}_{i-1,j} - P^{k-1}_{i+1,j}}{2\Delta x \Delta t}\right) \tag{16}$$

where i and j denote the space indices, k the time index, and $\Delta x$, $\Delta r$, and $\Delta t$ are the space and time mesh spacing, respectively. The time associated with equation (16) is defined as $t^{k+1} = t^k + \Delta t = (k + 1)\Delta t$. Equation (16) can be written in the form

$$P^{k+1}_{i,j} - 2P^{k}_{i,j} + P^{k-1}_{i,j} = \alpha \Psi_q \qquad (q = 1) \qquad (17)$$

where

$$\alpha = \frac{\Delta t^2}{\eta_r^2 \Delta x^2} \qquad (18)$$

In this case, $\Psi_q$ represents all the remaining difference terms on the right hand side of the equation. The subscript q stands for the cells shown in figure 1. In this case, q equals one for the central cell.

For ease in bookkeeping, $\Psi_q$ is broken down as follows

$$\Psi_q = a_q P^{k}_{i-1,j} + b_q P^{k}_{i,j-1} + c_q P^{k}_{i,j} + d_q P^{k}_{i,j+1} + e_q P^{k}_{i+1,j} + f_q P^{k+1}_{i,j} + g_q P^{k-1}_{i,j} + h_q P^{k+1}_{i-1,j} + i_q P^{k-1}_{i+1,j} \qquad (19)$$

Substituting equation (19) into equation (17) and solving for the pressure $P^{k+1}_{i,j}$, yields

$$P^{k+1}_{i,j} = \frac{\alpha}{\left[1 - \alpha f_q\right]} \left[a_q P^{k}_{i-1,j} + b_q P^{k}_{i,j-1} + \left(c_q + \frac{2}{\alpha}\right) \times P^{k}_{i,j} + d_q P^{k}_{i,j+1} + e_q P^{k}_{i+1,j}\right] - \left[\frac{1 - \alpha g_q}{1 - \alpha f_q}\right] P^{k-1}_{i,j} + \left[\frac{\alpha}{1 - \alpha f_q}\right] \times \left[h_q P^{k+1}_{i-1,j} + i_q P^{k-1}_{i+1,j}\right] \qquad (20)$$

The coefficients are listed in table I.

Equation (20) is an algorithm which permits marching out solutions from known values of pressure at times associated with k and k-1. The term $P^{k+1}_{i-1,j}$ is also a known quantity. At i = 2, the value of $P^{k+1}_{i,j}$ is known from the source condition, equation (7). At i = 3, the value of $P^{k+1}_{2,j}$ is known from the previous calculation at i = 2. Thus, the solution starts at the spatial position i = 2 and proceeds outward to i = I. The procedure is explicit since all the past values of $P^k$ are known as the new values of k + 1 are computed. For the special case at t = 0, the values of the pressure associated with the k-1 value are zero from the assumed initial condition.

Boundary Condition (Cells No. 2 to 6)

The expressions for the difference equations at the boundaries are complicated by the impedance condition and the change in area of cells no. 2 to 6 in figure 1. The governing difference equations can be developed by an integration process in which the wave equation (eq. (5)) is integrated over the area of the cells and time:

$$\int_{t-\Delta t/2}^{t+\Delta t/2} \iint_{\text{Cell area}} \eta_r^2 \frac{\partial^2 P}{\partial t^2} \, dx dr dt = \int_{t-\Delta t/2}^{t+\Delta t/2} \iint_{\text{Cell area}} \left[(1 - M^2) \frac{\partial^2 P}{\partial x^2} + \frac{\partial^2 P}{\partial r^2} + \frac{1}{r} \frac{\partial P}{\partial r} - \frac{m^2}{r^2} P - 2\eta_r M \frac{\partial^2 P}{\partial x \partial t}\right] dx dr dt \qquad (21)$$

The procedure for the temporal and spatial integration over the cell area is documented in reference 12, and therefore will not be presented herein. However, some extra steps that were not presented in reference 12 are listed in the Appendix of this paper.

The finite-difference approximation for the various cells shown in figure 1 are identical to equation (20) with the various cell coefficients listed in table I. Cells 3 and 6 have not been evaluated since the pressure at the centerline is equal to zero for spinning modes.

Spatial Mesh Size

The mesh spacing $\Delta x$ and $\Delta r$ must be restricted to small values to reduce the truncation error. To resolve the oscillatory nature of the pressure, the required number of grid points in the axial direction suggested in reference 1 was

$$I \geq \frac{12 \, L^*/r_o^*}{\lambda} \qquad (22)$$

where $\lambda$ is the axial wavelength of the sound. For spinning mode propagation in a semi-infinite hard cylindrical duct, $\lambda$ equals

$$\lambda = \frac{1 - M^2}{\eta_r(\beta - M)} \qquad (23)$$

therefore

$$I \geq 12\eta_r L^*/r_o^* \frac{(\beta - M)}{(1 - M^2)} \qquad (24)$$

Similarly, the number of points used in the r direction is[12]

$$J = 12\eta_r \qquad (25)$$

## Stability

In the explicit time marching approach used here, round-off errors can grow in an unbounded fashion and destroy the solution if the time increment $\Delta t$ is too large or the iteration scheme is improperly posed. In the present paper, numerical experimentation was used to determine the time increment $\Delta t$ for which the explicit solution remained stable. The initial guess for the time increment was based on the following equation developed in reference 13 for plane wave propagation in straight ducts:

$$\Delta t \leq \eta_r \frac{\Delta x(1 - |M|)}{\sqrt{1 + (\Delta r/\Delta x)^2}} \qquad (26)$$

## Steady State Pressures

In the sample problems to be presented in the next section, the time dependent results will be compared to the results of the steady harmonic solutions[14] (p. 509). The purpose of this section is to show the rational for constructing a steady state solution from the time-dependent results.

## Steady Harmonic Solution

The steady acoustic pressure $p(x,r)$ is defined as the solution to equation (5) when the pressure is assumed to be a simple harmonic function of time. For a semi-infinite hard wall circular duct with transmission of a single spinning mode, the analytical solution for $p_{m\,n}(x,r)$ is

$$p_{m\,n}(x,r) = J_m(\omega_{m\,n} r) e^{\frac{-i2\pi\eta_r(\beta - M)x}{1-M^2}} \qquad (x > 0) \qquad (27)$$

where $\beta$ is given by equation (12). In the next section of the present paper, the transient solution to the semi-infinite hard wall duct will be compared to equation (27).

## Transient Solution

Although multiple values of pressure are calculated at each time step, only the latest value values (k, k-1) need to be stored. After the initial transient has died out (checked numerically), the time dependent results can be compared to the "steady" state results (eq. (27)) simply by dividing by $e^{i2\pi t}$, that is,

$$p(x,r) = \frac{P(x,r,t)}{e^{i2\pi t}} \qquad (28)$$

The bookkeeping and graphical output is held to a minimum by the use of equation (28).

## Sample Calculations

In two sample problems to follow, the time-dependent results will be compared to the results of the steady harmonic solution given by equation (27).

## Zero Mach Number

Numerical and analytical values of the "steady" pressure $p(x,r)$ are computed for the case of a hard wall infinite duct with an $m = 3$ spinning mode. The calculation was made with a length to radius ratio of 1 and dimensionless frequencies of $\eta_r = 2$, 1, and 0.7. The analytical and numerical values of the acoustic pressure profiles along the duct wall ($r = 1$) are shown in figures 2(a), (b), and (c). As seen in figure 2, the steady and time-dependent analyses are in good agreement.

The cut-off frequency for the (3,0) mode is 0.66854. For $\eta_r = 0.5$, the numerical solution as formulated did not converge to the analytical solution. The numerical solution oscillated about the analytical solution. Therefore, at the present time, the numerical procedure can only be applied to propagating acoustic modes.

## Finite Mach Number

As another example of the time-dependent analysis, numerical and analytical values of the "steady" pressure $p(x,r)$ are computed at $\eta_r = 1$ but with uniform Mach numbers of +0.5 and -0.5. The analytical and numerical values of the acoustic pressure are shown in figures 3(a) and (b). As seen in figure 3, agreement between the analytical and numerical theory is good.

## Conclusions

A time dependent numerical procedure was developed for no flow and plug flow in a cylindrical duct. This explicit time marching technique was found to be stable for propagating acoustic modes with or without flow. For nonpropagating (cut-off) acoustic modes, however, the time dependent solution oscillates about the correct solution. This will ultimately have to be resolved since cut-off modes will be encountered in real problems. In the mean time, the steady state numerical techniques can be conveniently employed near cut-off. Because of the relatively long axial wave length near cut-off (see fig. 2(c)), the required number of grid points (or elements) is relatively small.

By eliminating large matrix storage requirements, numerical calculations of high sound frequencies in turbojet inlets are now possible. Because manipulation of matrices is omitted, the time dependent approach is relatively easy to program and debug.

## Appendix

### Finite-Difference Equations at Boundary

The derivation of the difference equations for the boundary cells was presented in reference 12. However, some additional terms appear in this paper which were not covered in reference 12. The treatment of these new terms are now considered.

**Mixed Derivative**

$$-2\eta_r M \int_{t-\Delta t/2}^{t+\Delta t/2} \iint_{\substack{\text{Cell}\\ \text{area}}} \frac{\partial^2 p}{\partial x \partial t}\, dx dr dt$$

$$= -2\eta_r M \overline{\frac{\partial^2 p}{\partial x \partial t}} \int_{t-\Delta t/2}^{t+\Delta t/2} \iint_{\substack{\text{Cell}\\ \text{area}}} dx dr dt \qquad (A1)$$

$$= -2\eta_r M \overline{\frac{\partial^2 p}{\partial x \partial t}}\, \Delta t \iint_{\substack{\text{Cell}\\ \text{area}}} dx dr \qquad (A2)$$

where from reference 15, p. 884, formula 25.3.27

$$\overline{\frac{\partial^2 p}{\partial x \partial t}}$$

$$= \frac{p^{k+1}_{i,j} + p^{k}_{i-1,j} + p^{k}_{i+1,j} + p^{k-1}_{i,j} - 2p^{k}_{i,j} - 2p^{k+1}_{i-1,i} - p^{k-1}_{i+1,j}}{2\Delta x \Delta t} \qquad (A3)$$

The area integral in equation (A2) will be $\Delta x \Delta r/2$ for Cells 2, 3, and 4, and $\Delta x \Delta r/4$ for Cells 5 and 6.

**Spinning Term**

$$-\int_{t-\Delta t/2}^{t+\Delta t/2} \iint_{\substack{\text{Cell}\\ \text{area}}} \frac{m^2}{r^2} P dx dr dt$$

$$= -\frac{m^2}{r_j^2} p^{k}_{i,j} \int_{t-\Delta t/2}^{t+\Delta t/2} \iint_{\substack{\text{Cell}\\ \text{area}}} dx dr dt \qquad (A4)$$

$$= -\frac{m^2}{r_j^2} p^{k}_{i,j}\, \Delta t \iint_{\substack{\text{Cell}\\ \text{area}}} dx dr \qquad (A5)$$

**References**


1. Baumeister, K. J. and Bittner, E. C., "Numerical Simulation of Noise Propagation in Jet Engine Ducts," NASA TN D-7339, 1973.
2. Baumeister, K. J. and Rice, E. J., "A Difference Theory for Noise Propagation in an Acoustically Lined Duct with Mean Flow," Aeroacoustics: Jet and Combustion Noise; Duct Acoustics, edited by H. T. Nagamatsu, J. V. O'Keefe, and I. R. Schwartz, Progress in Astronautics and Aeronautics Series, Vol. 37, American Institute of Aeronautics and Astronautics, New York, 1975, pp. 435-453.
3. Goldstein, M. E., Aeroacoustics, McGraw-Hill, New York, 1976.
4. Beaubien, M. J. and Wexler, A., "Iterative, Finite Difference Solution of Interior Eigenvalues and Eigenfunctions of Laplace's Operator," Computer Journal, Vol. 14, Aug. 1971, pp. 263-269.
5. Quinn, D. W., "A Finite Element Method for Computing Sound Propagation in Ducts Containing Flow," AIAA Paper 79-0661, Mar. 1979.
6. Browne, B. T. and Lawrenson, P. J., "Numerical Solution of an Elliptic Boundary-Value Problem in the Complex Variable," Institute of Mathematics and its Applications, Vol. 17, (3), 1976, pp. 311-327.
7. Baumeister, K. J., "Analysis of Sound Propagation in Ducts Using the Wave Envelope Concept," NASA TN D-7719, 1974.
8. Baumeister, K. J., "Finite-Difference Theory for Sound Propagation in a Lined Duct with Uniform Flow Using the Wave Envelope Concept," NASA TP-1001, 1977.
9. Baumeister, K. J., "Optimized Multisectioned Acoustic Liners," AIAA Paper 79-0182, Jan. 1979.
10. Baumeister, K. J., "Numerical Spatial Marching Techniques for Estimating Duct Attenuation and Source Pressure Profiles," NASA TM-78857, 1978.
11. Baumeister, K. J., "Numerical Spatial Marching Techniques in Duct Acoustics," Acoustical Society of America, Journal, Vol. 65, Feb. 1979, pp. 297-306.
12. Baumeister, K. J., "Time Dependent Difference Theory for Noise Propagation in Jet Engine Ducts," AIAA Paper 80-0098, Jan. 1980.
13. Baumeister, K. J., "A Time Deperdent Difference Theory for Sound Propagation in Ducts with Flow," NASA TM-79302, 1979.
14. Morse, P. M. and Ingard, K. U., Theoretical Acoustics, McGraw Hill, New York, 1968.
15. Abramwitz, M. and Stegun, I. A., eds., Handbook of Mathematical Functions with Formulas, Graphs and Mathematical Tables, National Bureau of Standards, Applied Mathematics Series,55, 1964.
16. Tag, I. A. and Lumsdaine, E., "An efficient Finite Element Technique for Sound Propagation in Axisymmetric Hard Wall Ducts Carrying High Subsonic Mach Number Flows," AIAA Paper 78-1154, July 1978.

TABLE I. - CELL SUMMARY

| Cell number, q | Difference elements | | | | | | | | |
|---|---|---|---|---|---|---|---|---|---|
| | $a_q$ | $b_q$ | $c_q$ | $d_q$ | $e_q$ | $f_q$ | $g_q$ | $h_q$ | $i_q$ |
| 1 | $(1 - M^2)\left(\frac{\Delta r}{\Delta x}\right)^2 - A$ | $1 - \frac{\Delta r}{2r_j}$ | $-2\left[1 + (1 - M^2)\left(\frac{\Delta r}{\Delta x}\right)^2\right] + 2A - \left(\frac{m\Delta r}{r_j}\right)^2$ | $1 + \frac{\Delta r}{2r_j}$ | $(1 - M^2)\left(\frac{\Delta r}{\Delta x}\right)^2 - A$ | -A | -A | +A | +A |
| 2 | $a_1$ | $2b_1$ | $C_1 + \frac{\Delta r}{r_j}$ | 0 | $e_i$ | $f_1$ | $g_1$ | $h_1$ | $i_1$ |
| 3 | -------- | ------- | ------- | ----- | ------ | ------ | ------ | ---- | ----- |
| 4 | $2(1 - M^2)\left(\frac{\Delta r}{\Delta x}\right)^2$ | $b_1$ | $-2\left[1 + (1 - M^2)\left(\frac{\Delta r}{\Delta x}\right)^2\right] - 2B - \left(\frac{m\Delta r}{r_j}\right)^2$ | $d_1$ | 0 | -E + B | +E + B | 0 | 0 |
| 5 | $a_4$ | $2b_1$ | $C_4 + \frac{\Delta r}{r_j}$ | 0 | 0 | $f_4$ | $g_4$ | 0 | 0 |
| 6 | -------- | ------- | -------- | ----- | ------ | ------ | ------ | ---- | ----- |

$A = \left(\frac{\Delta r^2}{\Delta x \Delta t}\right)\eta_r M$; $B = 2\left(\frac{\Delta r}{\Delta t}\right)^2 \frac{\eta_r^2 M}{\zeta_M}$ ; $E = \left(\frac{\Delta r^2}{\Delta x \Delta t}\right) \frac{\eta_r}{\zeta_M} (1 - M^2)$

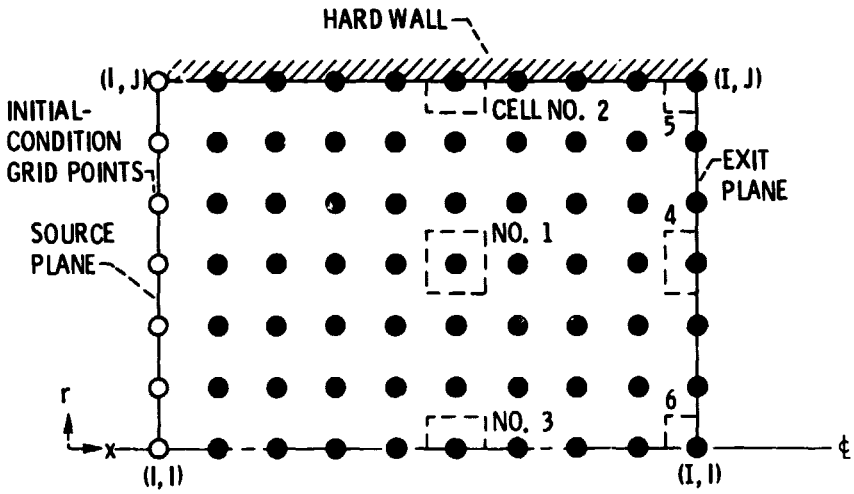


Figure 1. - Grid-point representation of cylindrical flow duct.

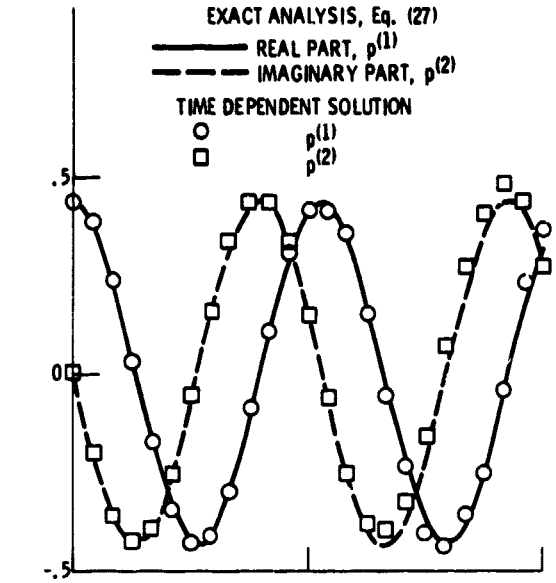


(a) FREQUENCY $\eta_r = 2$, $\Delta t = 0.006526$, $t = 3.008$.

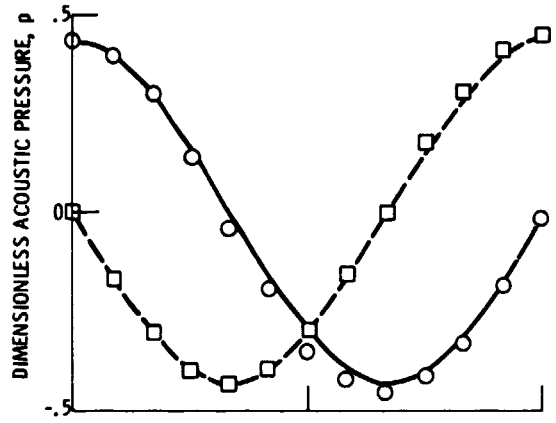


(b) FREQUENCY $\eta_r = 1.0$, $\Delta t = 0.00444$, $t = 3.006$.

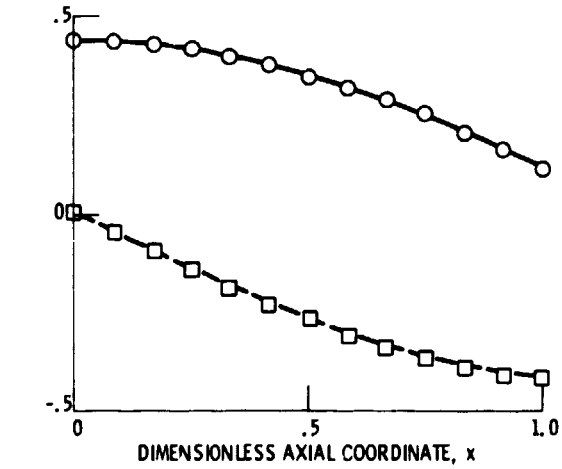


(c) FREQUENCY $\eta_r = 0.7$, $\Delta t = 0.003108$, $t = 10.70$.

Figure 2. - Analytical and numerical pressure profiles for spinning wave propagation in an infinite hard wall duct ($m = 3$, $n = 0$, $\alpha_{30} = 4.20119$, $J = 20$, $r = 1$).

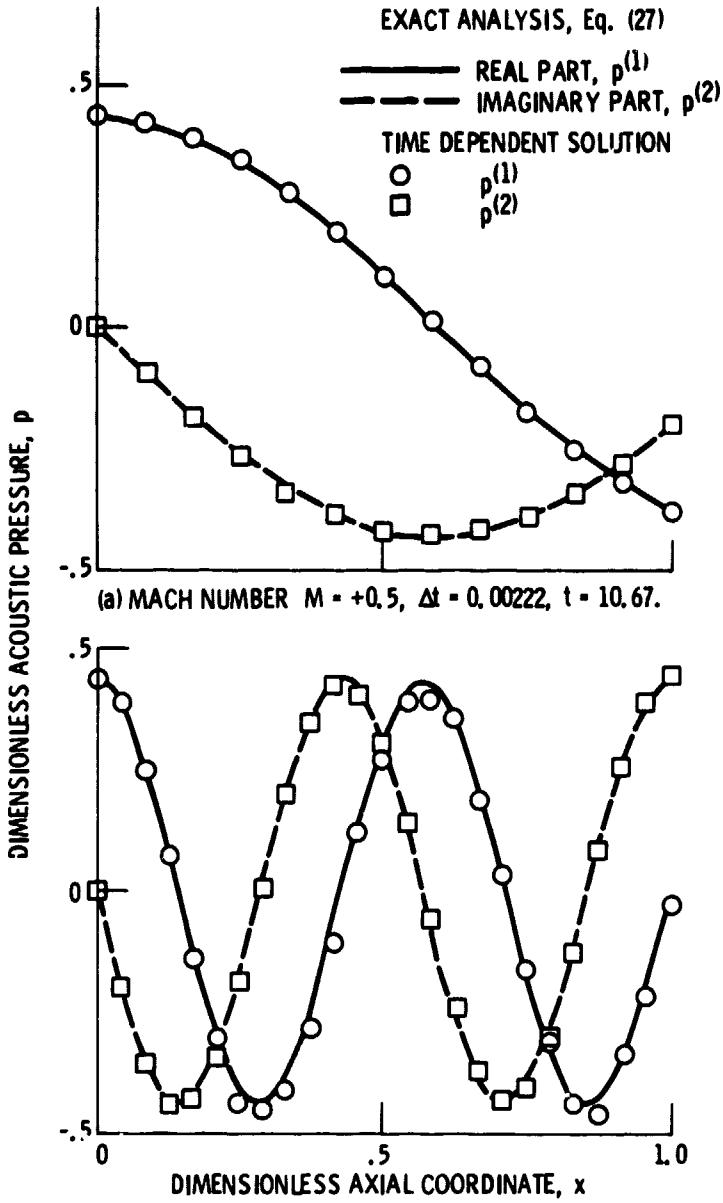


(a) MACH NUMBER M = +0.5, $\Delta t$ = 0.00222, t = 10.67.

(b) MACH NUMBER M = -0.5, $\Delta t$ = 0.001631, t = 4.002.

Figure 3. - Analytical and numerical pressure profiles for spinning wave propagation in an infinite hard wall duct with flow (m = 3, n = 0, $\alpha_{30}$ = 4.20119, J = 20, r = 1, and $\eta_r$ = 1).